Grid Generation and Adaptation for the Direct Simulation Monte Carlo Method

David P. Olynick*
North Carolina State University, Raleigh, North Carolina
James N. Moss†
NASA Langley Research Center, Hampton, Virginia
and
H. A. Hassan‡
North Carolina State University, Raleigh, North Carolina

A grid generation and adaptation procedure based on the method of transfinite interpolation is incorporated into the direct simulation Monte Carlo method of Bird. In addition, time is advanced based on a local criterion. The resulting procedure is used to calculate steady flows past wedges and cones. Five chemical species are considered. In general, the modifications result in a reduced computational effort. Moreover, the results suggest that the simulation method is time-step dependent if requirements on cell sizes are not met.

Introduction

THE direct simulation Monte Carlo (DSMC) method of Bird[1] has matured in the last few years to the point where calculation of complex flows has become almost routine.[2] Current research has focused on advanced applications such as aeroassisted orbital transfer vehicles, transatmospheric vehicles, and hypersonic aircraft. These vehicles encounter a broad range of flight conditions varying from continuum to rarefied flows. The DSMC method has been primarily used to investigate flow situations in which the assumptions of continuum methods become invalid, i.e., in the transitional and free molecule flow regimes. However, there is interest in comparing the continuum and Monte Carlo approaches in situations where both are applicable.

Computationally, for local Knudsen numbers of unity and higher, the particle approach is the only applicable method.[3] Consequently, Monte Carlo procedures such as DSMC have been developed to numerically simulate these problems. The major computational assumption of the DSMC procedure is the uncoupling of the molecular motion and collisions over a small local time interval Δt_m and the discretization of physical space into cells.[1] The successful application of the method requires a Δt_m, which is less than the local collision time and cell sizes of the order of a third of the local mean free path. The local properties are not known a priori. Thus, the grid generation procedure is necessarily iterative.

Solutions based on the Navier-Stokes equations are, in general, Reynolds number and grid dependent. Therefore, a meaningful comparison of continuum and Monte Carlo solutions requires that the same grid be used for both calculations. Moreover, because grid generation for complex shapes is a major undertaking, it is desirable to use a grid generation procedure that lends itself to the unique requirements of both the Navier-Stokes and the DSMC in two and three dimensions.

One of the objectives of this study, therefore, is to adapt the concept of transfinite interpolation developed by Ericksson[4] for wings and other three-dimensional configurations into the DSMC procedure. In addition, a grid adaptation procedure is developed to insure that cell size requirements of the DSMC are met. Finally, in order to obtain accurate steady-state solutions in the shortest possible computational time, the concept of a local Δt_m for each cell at each time step is implemented.

The above changes were incorporated into a code developed by Bird and used by Cuda and Moss[5,6] to study hypersonic flow past blunt wedges and cones at altitudes from 70–90 km. The paper examines the effects and benefits of the various changes indicated above. Comparisons are made with the results of Refs. 5 and 6 for 5-deg blunt wedges and cones at various altitudes.

Formulation of the Problem

The uncoupling of collisions and movement of the molecules over a short time interval Δt_m and the discretization of physical space into small cells are the major computational assumptions of the DSMC method. To satisfy the criteria for uncoupling, a Δt_m must be less than the local average collision time, i.e., $\Delta t_m < 1/\upsilon$, where υ is the local average collision frequency. For unsteady flow, one Δt_m is used throughout flowfield. On the other hand, if the boundary conditions are such that the flow is steady, then the computational effort can be facilitated by subdividing computational domain into an arbitrary number of regions. The Δt_m are constant in each region and can be different in different regions. The number of regions in the flow is usually small when compared with the number of cells. Usually, the value of Δt_m is chosen in such a way that the requirement $\Delta t_m < 1/\upsilon$ is met in each cell of the region. Because of this, the resulting Δt_m are necessarily conservative.

A cell network is generated for the sampling of flow properties and for the selection of collision partners. The collision partners are chosen statistically from within the cell independently of their physical location. A cell size is chosen so that changes in flow properties across a given cell are small.[7] Generally, a cell size is on the order of one-third of the local mean free path λ in the direction of primary gradients.

Received May 19, 1988; presented as Paper 88-2734 at the 23rd AIAA Thermophysics, Plasmadynamics, and Lasers Conference, San Antonio, TX, June 22–29, 1988; revision received Dec. 16, 1988.
Copyright © 1988, American Institute of Aeronautics and Astronautics, Inc. All Rights Reserved.

*Research Assistant, Mechanical and Aerospace Engineering. Student Member AIAA.
†Research Engineer, Aerothermodynamics Branch, Space Systems Division. Associate Fellow AIAA.
‡Professor, Mechanical and Aerospace Engineering. Associate Fellow AIAA.

Another important DSMC parameter is the scaling factor between computational molecules and real molecules F_{num}. Since it is computationally impossible to simulate all the molecules in an actual flow, each computational molecule represents a specified number of physical molecules. A typical range of F_{num} is $10^{10}-10^{15}$. F_{num} is important because it controls the distribution of computational molecules within the grid. To maintain realistic collision rates it is desirable to have 20–30 computational molecules in each cell.[1] In typical applications, the number density may vary several orders of magnitude within the flowfield.[6] Therefore, it is desirable to have a variable F_{num}. F_{num} like Δt_m is constant within a region. Furthermore, to conserve mass across region boundaries in the flow the ratio $F_{\text{num}}/\Delta t_m$ must be the same for all regions. Therefore, F_{num} and Δt_m are selected subject to constraints previously mentioned and the condition that $F_{\text{num}}/\Delta t_m$ is the same throughout the flowfield.

F_{num} determines the number of computational molecules. Its value may be adjusted to increase or decrease these molecules. A sample may be generated by simulating a large number of molecules for a short period of time or a small number of molecules for a large period of time. Both methods yield identical results.[1] Therefore, any value of $F_{\text{num}}/\Delta t_m$ can be chosen as long as the constraints on the number of molecules per cell and the time step are satisfied.

The cell size Δt_m and F_{num} are critical to the solution of a DSMC calculation.[7] First, an initial region and cell grid structure are generated. Second, assumed values of F_{num} are chosen for each region; Δt_m are then estimated subject to the constraint that $\Delta t_m/F_{\text{num}}$ be the same for all regions. Finally, the above parameters are iteratively modified until an acceptable number of computational molecules, cell size distribution, and Δt_m are obtained. Thus, the necessary series of iterations can be long and time-consuming.

Grid Generation

In this study a grid generation method based on the concept of transfinite interpolation developed by Ericksson[4] for wings and other three-dimensional configurations is introduced into the DSMC procedure. The method is algebraic and is capable of generating single-block mappings with geometry data specified at the boundaries of the computational domain. Thus, it is very inexpensive in terms of computer cost and is conceptually simple. Furthermore, the method can be applied to continuum and DSMC calculations. Therefore, in future applications it will be possible to make direct comparisons of continuum and DSMC flow solutions on identical grids. A more detailed description of this method is presented in the Appendix of this paper.

Before the implementation of the above procedure can be presented, it is necessary to describe the current DSMC grid generation scheme. The flowfield is divided into a number of arbitrary regions. Along the boundaries of these regions point distributions are generated and connected to form cells. However, the point distributions for each region are chosen independently. Thus, the method can cope with a grid that can be discontinuous across regions and that can have large variations in cell sizes.

The grid generation scheme introduced in this paper offers the following simplifications. The grid is generated from the point distributions along the flowfield boundaries including normal derivatives at the surface. This substantially reduces the amount of input necessary for DSMC initialization and simplifies later grid modifications. Second, the grid cell structure varies smoothly. A possible drawback of this method is control of interior cell sizes[4] that are far from the flowfield boundaries. However, this did not prove to be a problem for the flows considered in this study.

Grid Adaption

The purpose of grid adaptation is to generate a point or cell distribution along the stagnation streamline and surface that reflects flowfield gradients. The objective of the adaptation scheme employed is twofold. The first is to place grid points where needed to obtain an accurate solution with a minimum grid size. The second is to ensure that cell sides are of the order of $\lambda/3$, where λ is the local mean free path. Because

$$\lambda \alpha \frac{1}{n} \tag{1}$$

where n is the number density, the above requirement can be stated as

$$\Delta x_i \simeq \frac{\lambda}{3} \alpha \frac{1}{n}$$

or

$$n\, \Delta x_i \alpha \text{ const} \tag{2}$$

where Δx_i is a cell side. Thus, the objective of the adaptation can be met by the equidistribution of $n\, \Delta x_i$.

The procedure for grid adaptation employed here is as follows. First, a grid is generated and used to calculate the flowfield. Generally, this initial grid is produced from considerations of the freestream Mach number and mean free path. When the flow is almost steady (e.g., $\Delta n/n < 1\%$), a number density distribution can be obtained from sampled flow properties. These values are spline-fitted to generate $n = n(s)$, where s is the distance along the boundary. From this distribution, the quantity

$$N = \int_0^{s_{\max}} n(s)\, \mathrm{d}s \tag{3}$$

is obtained. For a given s_i, an iterative procedure can be used to determine s_{i+1}, such that

$$\frac{N}{m} = \int_{s_i}^{s_{i+1}} n(s)\, \mathrm{d}s \tag{4}$$

where m is the number of cells along the chosen boundary. This produces a one-dimensional point distribution that can be used for grid generation. In general, this procedure can be applied in any flow direction. For this study, a point distribution was generated along the stagnation streamline and body surface. With the new grid, the flow solution can be recalculated and the adaptation procedure reapplied. This is done until a satisfactory cell distribution is obtained. In practice, two grid adaptations should be sufficient.

In the event that the initial grid is coarse, i.e., m in Eq. (3) is small, the resulting cell sizes may, even after adaptation, violate the grid size requirement indicated in Eq. (1). In this case, the grid size must be increased to conform to Eq. (1).

The benefits of this adaptation scheme are as follows. First, the procedure of choosing a point distribution along the region boundaries is automated. Second, the point distribution is based on a fundamental quantity of the flowfield, which is the number density. Finally, the method concentrates points where needed.

Local Time Step

The third modification introduced in this study is in the calculation of the local time step Δt_m. To uncouple the collision and movement routines, Δt_m must be less than the local average collision time $1/\upsilon$, where υ is the local collision frequency. The time step Δt_m for a rectangular cell aligned with the coordinate axes in a Cartesian coordinate system is given by

$$\Delta t_m = \min\left[\frac{\Delta x}{U_{\max}}, \frac{\Delta y}{V_{\max}}\right] \tag{5}$$

where U_{max}, V_{max} are the maximum (total) velocity components of the molecules that cross a cell during a movement step and Δx, and Δy are the cell length and width for each cell. However, to account for cell skewing, the following formula is used to calculate Δt_m:

$$\Delta t_m = \min\left[\frac{A_{cell}}{U_{max}\,\Delta y_h - V_{max}\,\Delta x_h}, \quad \frac{A_{cell}}{U_{max}\,\Delta y_v - V_{max}\,\Delta x_v}\right] \tag{6}$$

where

$$\Delta x_h = 0.5(x_2 + x_3 - x_1 - x_4)$$

$$\Delta y_h = 0.5(y_2 + y_3 - y_1 - y_4)$$

$$\Delta x_v = 0.5(x_1 + x_2 - x_3 - x_4)$$

$$\Delta y_v = 0.5(y_1 + y_2 - y_3 - y_4)$$

$$A_{cell} = 0.5|\boldsymbol{l} \times \boldsymbol{m}|$$

$$\boldsymbol{l} = \boldsymbol{i}(x_2 - x_4) + \boldsymbol{j}(y_2 - y_4)$$

$$\boldsymbol{m} = \boldsymbol{i}(x_1 - x_3) + \boldsymbol{j}(y_1 - y_3)$$

The x and y coordinates refer to the cell corners, which are numbered in a counterclockwise direction starting with x_1, y_1 in the bottom right corner. A_{cell} is the cell area, and U_{max} and V_{max} are the same as before. This formula results when the previously described rectangle is rotated through some angle, and the velocity components are recalculated to align them with the cell sides. However, for nonrectangular cells the above formula only approximately accounts for the effects of cell skewing.

The choice of Δt_m in this manner insures that a molecule will remain in a cell for at least one time step. Furthermore, Δt_m is always smaller than the local collision time. This can be shown in the following manner. The average collision frequency can be defined as

$$\upsilon = \frac{\bar{c}'}{\lambda} \tag{7}$$

where $\bar{c}'$ is the average thermal speed. If the smallest cell dimension is $\lambda/3$, then $\Delta t_m = \lambda/3U$, which must be less than $1/\upsilon$. In general, U_{max} or V_{max} is larger than the average thermal speed. Therefore,

$$\Delta t_m = \frac{\lambda}{3U} < \frac{\lambda}{\bar{c}'} = 1/\upsilon, \quad U = \max(U_{max}, V_{max}) \tag{8}$$

The new procedure permits a calculation of Δt_m in each cell. Since F_{num} can be calculated from Δt_m and the constant $\Delta t_m / F_{num}$, each cell in the modified DSMC procedure is treated like a region in the previous DSMC. Therefore, Δt_m and F_{num} are truly local flowfield parameters.

In summary, the benefits of the new Δt_m calculation procedure are as follows. First, an automated procedure is used to adjust Δt_m. Second, the procedure ensures that the uncoupling assumption is always satisfied. Finally, the calculated values of Δt_m and F_{num} are more representative of local flow conditions since they are adjusted on an individual cell basis rather than on a region basis.

Simulated Molecules

The implication of adaptation and time step on cell population is considered. Cell adaptation is determined by Eq. (2), and the requirement on cell time step is given by Eq. (4), which shows that

$$\Delta t_m \sim \Delta x$$

The number of simulated molecules in a cell N_m is determined from

$$N_m F_{num} \simeq n(\Delta x)^k \tag{9}$$

where k is the dimensions of the problem. Because $F_{num}/\Delta t_m$ is constant, Eq. (9) shows

$$N_m \sim n(\Delta x)^{k-1}$$

or, from Eq. (2)

$$N_m \sim n^{2-k} \tag{10}$$

The above relation shows that the simulated molecules are almost distributed equally amongst the cells for two-dimensional flow ($k = 2$), but will be concentrated in the high-density cells of the one-dimensional flow and in the low-density cells in three-dimensional flows. Thus, the current scheme results in an almost optimal distribution for two-dimensional flows and an improved distribution for three-dimensional flows.

Results and Discussion

The flows calculated in this study were for a two-dimensional cylindrically blunted 5-deg half-angle wedge with a nose radius of 0.0254 m and length of 0.2 m. Furthermore, an axisymmetric cone with the same dimension was calculated. Wedge solutions were obtained at altitudes of 80 and 90 km. The cone solution was for an altitude of 90 km. The freestream velocity was 7.5 km/s for all cases. These cases were chosen as a baseline for comparison with the traditional DSMC procedure. They are a representative sample of solutions generated in Refs. 5 and 6. All calculations presented here considered the five chemical species: N_2, O_2, NO, O, and N.

The first objective of this work is to demonstrate that the new procedure gives results that are as accurate as the traditional DSMC. Figure 1 shows the grid used in Ref. 5 to calculate the flow past a 5-deg blunted wedge at an altitude of 90 km. The calculations employed eight regions that are approximately parallel to the body. Figure 2, which has the same number of cells as Fig. 1, depicts the grid generated by

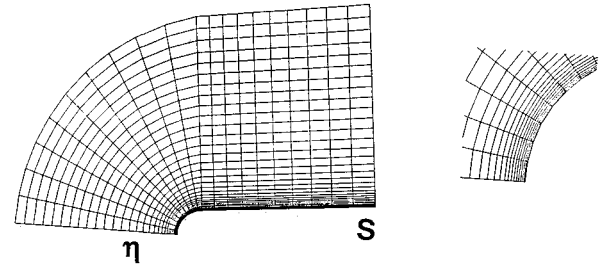

Fig. 1 Grid used in Ref. 5 for 5-deg wedge (90 km).

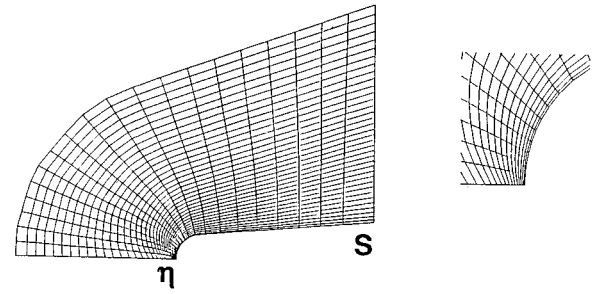

Fig. 2 Grid generated by transfinite interpolation.

the method of transfinite interpolation and adapted (twice) in the manner outlined above. Figure 3 compares the distributions along the surface (s distance along surface) of C_h the heat-transfer coefficient, C_p the pressure coefficient, C_f the skin-friction coefficient, and n the number density with those of Ref. 5. As is seen in the figure, good agreement is indicated. However, the computational time and effort required for each calculation are not equal. The Δt_m used in the traditional DSMC were about 1/10 of the values used for grid 2. This dictates longer computational times to obtain a grid-independent steady-state solution. The reduction in effort is a result of the highly automated nature of grid adaptation and generation.

The mean free path decreases with altitude, and more stringent requirements are placed on the grid spacing normal to the body. In order to assess the effectiveness of the grid adaptation scheme, flow past a 5-deg wedge at an altitude of 80 km is considered next. Starting with a coarse 45 × 40 grid (45 refers to cells along stagnation streamline, and 40 refers to cells along the body), a solution was obtained. As is seen in Fig. 4, a plot of $\Delta\eta/\lambda$ vs s, where the $\Delta\eta$ are the heights of the first row of cells along the body, shows that the grid does not meet the requirements of the DSMC. The results were used to adapt a 60 × 30 grid. As is seen from Fig. 4, $\Delta\eta/\lambda$ for this grid are marginal. The figure also displays $\Delta\eta/\lambda$ for the 70 × 20 grid used in Ref. 5. Figure 5 presents the comparison of the computed flow characteristics with those obtained in Ref. 5. As is seen from the figure, some discrepancy exists in some of the results around the stagnation point and shoulder (good agreement is obtained for C_p, not shown). The new calculation procedure is compared with the standard procedure for the 70 × 20 grid used in Ref. 5. The pressure coefficient and number density distributions are in good agreement with the results of Ref. 5. However, as is seen from Fig. 6, some discrepancy exists in C_h and C_f. Figure 7 shows the influence of reducing Δt_m by a factor of four for the 60 × 30 grid. Again, a discrepancy exists between these results and those of Ref. 5.

All the differences in the results indicated in Figs. 6 and 7 are a result of differences in the manner in which Δt_m is chosen. Upon further examination, it became evident that some cells in the flowfield do not meet the requirements indicated in Eq. (1). Therefore, if the criterion regarding cell sizes is not met throughout, the method will be Δt_m-dependent. This confirms an earlier result by Bird.[8]

As a last comparison, the flow was calculated for a 5-deg cone at an altitude of 90 km. The results were generated using the adapted grid shown in Fig. 2. Good agreement for C_f, C_h, C_p, and n vs s is indicated. However, as is seen from Fig. 8, which shows C_{O_2} and C_{N_2} vs η or the mass fractions of O_2 and N_2 vs the distance along the stagnation streamline, the results of Ref. 6 are not smooth. The smooth distribution

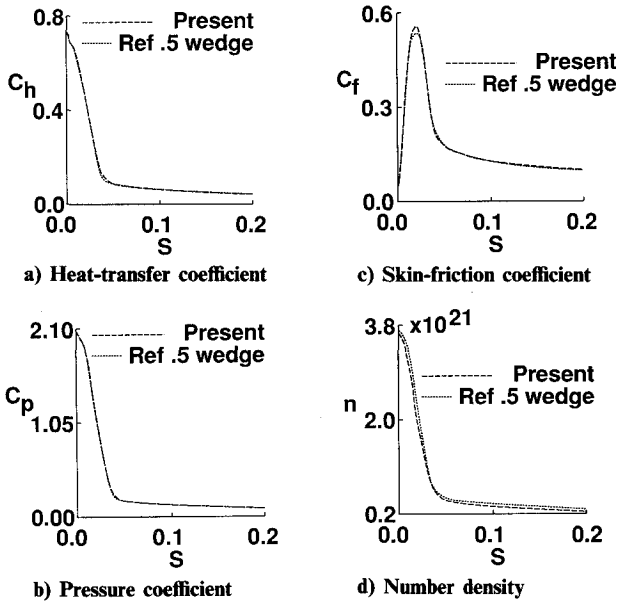

Fig. 3 Surface properties for 5-deg wedge (90 km).

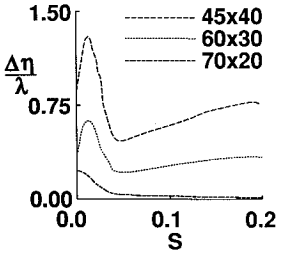

Fig. 4 Distribution of heights of first row of cells along surface.

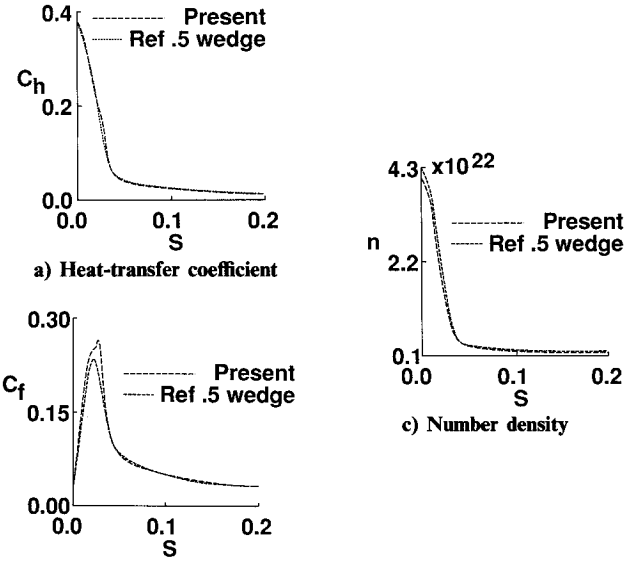

Fig. 5 Comparison of surface properties for 5-deg wedge (80 km and a grid of 60 × 30).

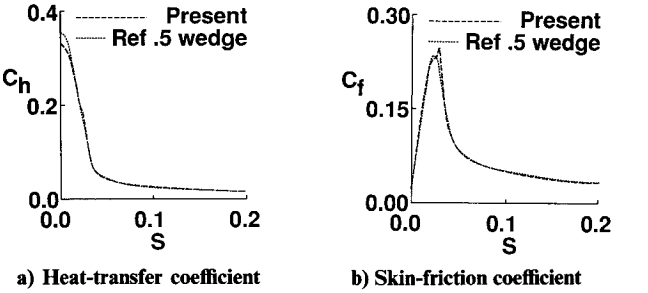

Fig. 6 Comparison of surface properties for 5-deg wedge (80 km and a grid of 70 × 20).

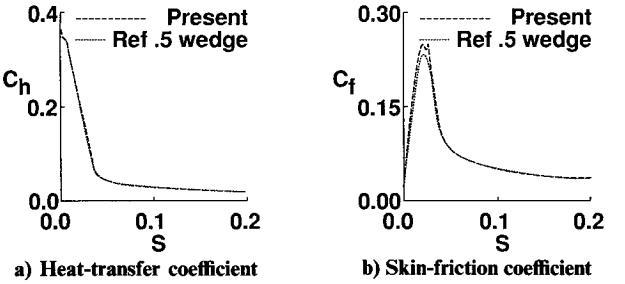

Fig. 7 Effect of reduced time step on surface properties for 5-deg wedge (80 km).

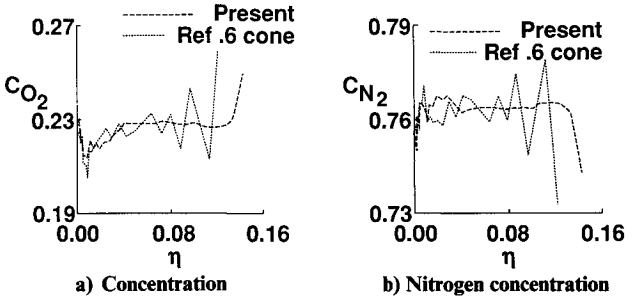

Fig. 8 Concentration of O_2 and N_2 along stagnation streamline.

obtained by the present method is a result of the manner in which Δt_m is selected.

Concluding Remarks

In this study changes were introduced into the DSMC method in order to simplify the grid generation and computation procedure. This modified DSMC method was used to calculate hypersonic flow past blunt wedges and cones and to compare them with existing DSMC solutions. The results of these calculations show the following:

1) The grid adaptation and generation procedure introduced here results in a reduction of the overall computational effort because of the ease of generating and modifying grids.

2) Use of a local time step for each step results in a reduction of the overall computational time for steady-state calculations. The reduction is user-dependent. This is because a user may select a Δt_m much less than is required by Eq. (6); in such a case the reduction would be substantial. On the other hand a user may select a Δt_m consistent with Eq. (6); in such a case the reduction would be minimal.

3) Smoothly varying grids Δt_m and F_{num} help reduce oscillations, especially for axisymmetric flows.

4) The results of DSMC flow calculations are grid-independent if the calculation satisfies the computational assumptions of the DSMC method. On the other hand they are Δt_m dependent if requirements on cell sizes are not met.

Acknowledgment

This work is supported in part by NASA's cooperative agreement NCCI-112 and the Hypersonic Aerodynamics Program Grant NAGW-1072 funded jointly by NASA, AFOSR, and ONR. The authors would like to thank Professors G. A. Bird and F. J. Brock for their guidance and advice. The section on simulated molecules was suggested by Dr. R. Daniel McGregor of TRW. The authors would like to express their appreciation for his constructive suggestions.

Appendix: Transfinite Interpolation Method

The grid generation method employed in this paper was developed by Ericksson[8] for surface-fitted mesh systems about two- and three-dimensional configurations. Application of the method requires parametric functions of x and y at the flowfield boundaries. From this information interior grid points can be quickly generated using the algebraic method of transfinite interpolation. Grid control is obtained using derivatives at the boundary surface and blending functions inherent in the method.

The application of the method involves the mapping of the flowfield boundaries to a rectangular computational domain. Let the coordinates of the computational domain be given by u and v. Then, the corners of the domain, starting in the bottom left corner and moving clockwise, are given by $(u_1,v_1),(u_1,v_2)(u_2,v_2),(u_2,v_1)$. The body surface is mapped to the side $v=v_1$, and the outer boundary is mapped to the side $v=v_2$. The boundaries between the body and outer boundary are mapped to the sides $u=u_1$ and $u=u_2$. Finally, the spacing in the computational domain Δu and Δv is unity.

It is assumed that the mapping function $f(u,v)=[x(u,v),y(u,v)]$ is known on the boundaries of the rectangle, i.e., the functions $f(u_1,v)$, $f(u_2,v)$, $f(u,v_1)$, and $f(u,v_2)$, which are one-dimensional point distributions for x and y, are known. Therefore, the problem consists of extending the mapping function $f(u,v)$ into the interior of the rectangle. Utilizing the known boundary information, including normal derivatives at the body surface, the following projections in the u and v directions are formed:

$$\pi_u f = f(u_1,v)\alpha_1(u) + f(u_2,v)\alpha_2(u)$$

and

$$\pi_{v_2} f = f(u,v_1)\beta_1(v) + \frac{\partial f(u,v)}{\partial v}\beta_2(v) + f(u,v_2)\beta_3(v)$$

with

$$\alpha_1(u_1)=1,\ \alpha_1(u_2)=0,\ \beta_1(v_1)=1,\ \beta_1'(v_1)=0,\ \beta_1(v_2)=0$$
$$\alpha_2(u_1)=0,\quad \alpha_2(u_2)=1,\quad \beta_2(v_1)=0,\quad \beta_2'(v_1)=1$$
$$\beta_2(v_2)=0,\quad \beta_3(v_1)=0,\quad \beta_3'(v_1)=0,\quad \beta_3(v_2)=1$$

The transfinite interpolation is obtained from the Boolean sum of these projections:

$$\begin{aligned}\pi_u \oplus \pi_v f = (\pi_u + \pi_v - \pi_u\pi_v)f &= f(u_1,v)\alpha_1(u) + f(u_2,v)\alpha_2(u)\\ &+ f(u,v_1)\beta_1(v) + \frac{\partial f(u,v)}{\partial v}\beta_2(v) + f(u,v_2)\beta_3(v)\\ &- f(u_2,v_1)\alpha_1(u)\beta_1(v) - f(u_2,v_1)\alpha_2(u)\beta_1(v)\\ &- f(u_1,v_2)\alpha_1(u)\beta_3(v) - f(u_2,v_2)\alpha_2(u)\beta_3(v)\\ &- \frac{\partial f(u_2,v_1)}{\partial v}\alpha_1(u)\beta_2(v) - \frac{\partial f(u_2,v_1)}{\partial v}\alpha_2(u)\beta_2(v)\end{aligned}$$

From this equation and the choice of the beta and alpha, it is evident that the scheme reproduces the flow boundaries at the edges of the (u,v) rectangle. Applying this formula, interior grid points are quickly generated from three basic components: the value of the mapping functions at that point, the value of the mapping functions at the rectangle corners, and the beta and alpha functions. The various alpha and beta can be chosen any function of u and v meeting the previously described conditions. This allows further control over the grid generation process. The values of alpha used in this paper are

$$\alpha_1(u) = \frac{u_2-u}{u_2-u_1}e^{-k\left(\frac{u-u_1}{u_2-u_1}\right)}, \qquad \alpha_2(u) = \frac{u-u_1}{u_2-u_1}e^{-k\left(\frac{u_2-u}{u_2-u_1}\right)}$$

The function in front of the exponent is the simplest function satisfying the restrictions on alpha. The exponent can be used to damp out the influence of the body surface and outer boundary on the interior grid. A large k leads to heavy damping, whereas $k=0$ results in no damping. The beta functions used are

$$\beta_1(v) = 1 - \left(\frac{v-v_1}{v_2-v_1}\right)^2$$

$$\beta_2(v) = \left[\frac{v-v_1}{v_2-v_1} - \left(\frac{v-v_1}{v_2-v_1}\right)^2\right](v_2-v_1)$$

$$\beta_3(v) = \left(\frac{v-v_1}{v_2-v_1}\right)^2$$

These are the simplest functions satisfying the previously described constraints on beta. More elaborate functions for

alpha and beta may be used allowing further control of the grid generation process.

The method of transfinite interpolation scheme can also be extended to three-dimensional configurations.[4] The algebra is more involved, but the procedure is similar to the one described above. Furthermore, an infinite number of surface derivatives can be added to the scheme, and the use of derivatives can be extended to the other boundaries.

References

[1]Bird, G. A., *Molecular Gas Dynamics*, Oxford Univ. Press, London, 1976.

[2]Bird, G. A., "Nonequilibrium Radiation During Re-entry at 10 km/sec," AIAA Paper 87-1543, 1987.

[3]Bird, G. A., "Monte Carlo Simulation of Gas Flows," *Annual Review of Fluid Mechanics*, Vol. 10, edited by M. D. Van Dyke et al., Annual Reviews, Inc. Palo Alto, CA, 1979, p. 11.

[4]Ericksson, L. E., "Generation of Boundary Conforming Grids Around Wing-Body Configurations Using Transfinite Interpolation," *AIAA Journal*, Vol. 20, Oct. 1982, pp. 1313–1320.

[5]Cuda, V., Jr., and Moss, J. N., "Direct Simulation of Hypersonic Flow Over Blunt Wedges," *Journal of Thermophysics and Heat Transfer*, Vol. 1, No. 2, April 1987, pp. 97–104.

[6]Cuda, V., Jr., and Moss, J. N., "Direct Simulation of Hypersonic Flows Over Blunt Slender Bodies," AIAA Paper 86-1348, June 1986.

[7]Moss, J. N. and Bird, G. A., "Direct Simulation of Transitional Flow for Hypersonic Re-entry Conditions," *Progress in Astronautics and Aeronautics: Thermal Design of Aeroassisted Orbital Transfer Vehicles*, Vol. 96, edited by H. F. Nelson, AIAA, New York, 1985, pp. 113–139.

[8]Bird, G. A., "Rarefied Hypersonic Flow Past a Slender Sharp Cone," *Rarefied Gas Dynamics*, Vol. 1, edited by O. M. Belotserkovskii, Plenum Press, New York, 1985, pp. 349–356.

From the AIAA Progress in Astronautics and Aeronautics Series

THERMOPHYSICS OF ATMOSPHERIC ENTRY—v. 82

Edited by T.E. Horton, The University of Mississippi

Thermophysics denotes a blend of the classical sciences of heat transfer, fluid mechanics, materials, and electromagnetic theory with the microphysical sciences of solid state, physical optics, and atomic and molecular dynamics. All of these sciences are involved and interconnected in the problem of entry into a planetary atmosphere at spaceflight speeds. At such high speeds, the adjacent atmospheric gas is not only compressed and heated to very high temperatures, but stongly reactive, highly radiative, and electronically conductive as well. At the same time, as a consequence of the intense surface heating, the temperature of the material of the entry vehicle is raised to a degree such that material ablation and chemical reaction become prominent. This volume deals with all of these processes, as they are viewed by the research and engineering community today, not only at the detailed physical and chemical level, but also at the system engineering and design level, for spacecraft intended for entry into the atmosphere of the earth and those of other planets. The twenty-two papers in this volume represent some of the most important recent advances in this field, contributed by highly qualified research scientists and engineers with intimate knowlege of current problems.

Published in 1982, 521 pp., 6×9, illus., $29.95 Mem., $59.95 List

TO ORDER WRITE: Publications Dept., AIAA, 370 L'Enfant Promenade, SW, Washington, DC 20024